U. S. Department of Commerce
National Bureau of Standards

Research Paper RP1823
Volume 39, September 1947

Part of the Journal of Research of the National Bureau of Standards

Shunts and Inductors for Surge-Current Measurements

By John H. Park

The special requirements that must be fulfilled by a shunt intended to be used in surge-current measurements are explained. A tubular shunt with coaxial potential leads that meets these requirements is described, and factors affecting its design are discussed. A theoretical derivation of the "skin effect" in this type of shunt at high frequencies is given in one of the appendices.

The advantages of using a mutual inductor for obtaining oscillograms of the rate of change of current during a surge are outlined, and several types of mutual inductors developed especially for this purpose are described. Theoretical derivations, given in the appendices, indicate that the concentric-tube mutual inductors described in this paper can be used to measure the high-frequency components of a current surge up to 70 megacycles with less than 10 percent error.

Several shunts and mutual inductors of the designs described in this paper were constructed for use in the high voltage laboratory at the National Bureau of Standards. Their complete description and oscillograms showing results obtained with them are included.

I. Introduction

Surge-current generators are widely used in high-voltage laboratories to simulate the heavy current component of a lightning discharge. They are regularly employed in testing protective devices that are intended to withstand lightning discharges and in determining the effects of heavy-current discharges on various materials and apparatus. In order to correlate the test results obtained in various laboratories, it is necessary to know the magnitude and wave-form of the surge current used in each test.

A generally accepted method of measuring heavy-current surges is to insert a shunt in the discharge circuit and to apply the voltage drop across this shunt, through a suitable cable, to the deflecting plates of a cathode-ray-oscillograph capable of recording the variation of this voltage with time. The over-all accuracy of this method is dependent upon the three components used in the measurement: the cathode-ray-oscillograph, the cable, and the shunt.

The development of the cathode-ray-oscillograph to its present state of efficacy has involved years of work of a large number of experimenters and theorists. At the present time there are several types of oscillographs having recording speeds and response accuracies suitable for surge measurements. In general they may be classified as (1) the high-voltage cold-cathode type with the recording film inside the vacuum chamber, (2) the hot-cathode type with the film inside the vacuum chamber, and (3) the hot-cathode sealed-tube type using a fluorescent screen photographed by means of an external camera. Results reported in the present paper were obtained using an oscillograph of the first type; however, with slight modifications in design constants the apparatus to be described would be equally suitable for use with other types of oscillographs.

In order to facilitate safety precautions and to allow one cathode-ray-oscillograph (CRO) to be used with any one of several surge generators, the oscillograph is usually located at some distance from the surge generator and its potential divider and/or shunt and a cable (40 to 100 ft. long) is used to connect them to the deflecting plates of the oscillograph. The purpose of this cable is to reproduce the voltage drop across the shunt, at the deflecting plates of the oscillograph without distortion, and it must not introduce other voltages by induction from nearby currents. The use of coaxial-type cables reduces inductive effects to a minimum, and when constructed with insulating material of low dielectric loss, such as polyethylene, coaxial cables are capable of transmitting all components of a surge up to at least 100 megacycles/sec over the distances required without significant attenuation. The terminations of the cable, at the shunt and at the oscillograph, are both important.

Various types of shunts have been used for measuring heavy-current surges [1,2,3],[1] and long before surge generators were in general use, the design of alternating current shunts to insure low residual inductance was given considerable attention [4,5]. Thus, the design of the shunts now in use at this laboratory for surge-current measurements is based on experience with shunts used for measuring large alternating currents as well as on subsequent experience in the field of surge-current measurement. The present paper will discuss the design of surge-current shunts, describe those constructed, and indicate the results obtained with them.

This paper will also describe a new design of mutual inductor for measuring rate of change of current. Because it tends to magnify the high frequency components in current waves it has been useful in their measurement.

II. Factors To Be Considered in the Design of a Shunt

1. Choice of the Best Type

In choosing the best type of design for a shunt to be used in measuring surge currents the three most important requirements are (1) the effective impedance considered as a 4-terminal network must be constant over as great a range in frequency as possible, (2) inductive effects of parts of the current circuit, other than the shunt, upon the potential-lead circuit of the shunt should be a minimum, and (3) it must be possible to connect the sheath of the cable from the shunt to the CRO, to ground at or near the shunt without introducing induced voltages in the shunt potential circuit (this is desirable to minimize the flow of ground currents in the sheath of the cable which might cause induced voltage at the CRO plates).

In order to determine compliance with requirement number one, the configuration of the shunt should preferably be such that its inductance and skin effect can be computed for as great a range in frequency as possible; otherwise the comparison of various types of shunts would require the actual construction of a large number with subsequent experimental comparisons. Two general types lend themselves to computations: (a) the concentric tubular and (b) the flat strip. Illustrations of these, giving the methods of attaching potential leads, are shown in figure 1. Another

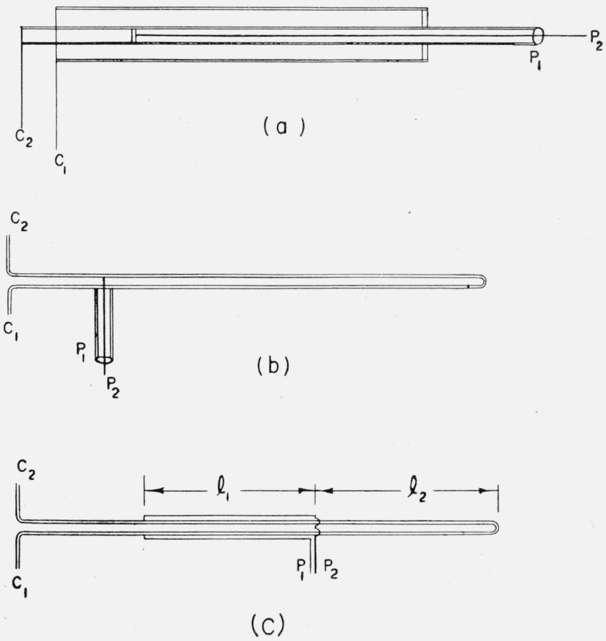

FIGURE 1.—*Three types of shunts whose inductance and skin effect can be computed.*

a, Concentric-tube shunt; *b*, flat-strip shunt; *c*, flat strip shunt with potential leads arranged to give minimum inductance.

type of shunt used by Bellaschi [1] in surge measurements consists of several twisted "hairpin" loops of resistance wire connected in parallel at the current terminals. This type of shunt has been found suitable for most surge-current measurements, but its inductance and skin effect cannot be accurately computed from theoretical formulas. An approximate theoretical computation by Brownlee [2] indicates that the twisted loop shunt would probably have a somewhat larger time constant than a flat strip shunt. Theoretical formulas for computing the inductance (assuming uniform distribution of current) and skin effect (for a limited frequency range) of the concentric tubular and flat strip shunts are

[1] Figures in brackets indicate the literature references at the end of this paper.

readily available.[2,3] As suggested by Silsbee [4] a strip shunt with potential leads attached as shown in figure 1, c, could be designed so as to have zero effective inductance by a suitable choice of values of l_1 and l_2. However, this arrangement of potential leads prevents the shunt from complying with requirement (3) above, as will be explained later, so it is not considered in the following comparison of coaxial tubular vs. flat-strip shunts.

To compare the constancy of effective impedance as frequency changes, for the tubular and flat-strip shunts, two typical designs of shunt were assumed and their inductance and skin effect computed from the formulas referred to above. A concentric tubular shunt (fig. 1, a) in which the resistance material was a CuNi alloy ($\rho=22.9\text{x}10^{-6}$ ohm cm) tube whose outside diameter was 0.25 in. and wall thickness was 0.008 in. was chosen as one example because such a tube was readily available for use in constructing a shunt. For comparison purposes a strip shunt was chosen whose thickness was the same as the wall thickness of the tube, whose width was the same as the circumference of the tube, and whose separation between strips was taken to be 0.01 in. (The shunt length does not affect these computations provided it is several times the largest transverse dimension.) The time constants for the shunts as obtained using the theoretical formulas assuming uniform distribution of current were (1) for tubular shunt $L/R=-0.0365\text{x}10^{-6}$; and (2) for strip shunt $L/R=0.218\text{x}10^{-6}$. The skin effects at $f=1$ megacycle as obtained from formulas given by Silsbee were (1) for tubular shunt $R/R_{dc}=0.959$; and (2) for the strip shunt $R/R_{dc}=0.955$. It must be remembered that these results do not give an accurate evaluation of the constancy of effective impedance at frequencies over 1 megacycle, because at such frequencies the skin effect causes a nonuniform distribution of current density over the thickness of the tube or strip, for which the theoretical formulas used in the above computation do not hold—no published theoretical formulas good at these high frequencies were known to the author. However, the above results should serve their purpose as a comparison between the two types of shunts. The tubular shunt has a much lower time constant than the strip shunt, which means that its reactance will be negligible over a higher frequency range. The skin effect at 1 megacycle appears to be the same for both shunts, but the formula used in obtaining the skin effect for the strip shunt neglects edge effects that are known to considerably increase [5] the skin effect at higher frequencies. Thus it would appear that the tubular shunt, as it has no edge effects, would have less change in effective resistance at the higher frequencies than the strip shunt. A decrease in both inductance and skin effect could be obtained by using a thinner strip or a thinner walled tube, but this cannot be carried to extremes because of the heat capacity requirements of the shunt, which will be discussed later; any improvement made by this means in the strip shunt could probably also be made in the tubular shunt, though possibly not to the same extent. Thus, it would appear that either a coaxial tubular shunt or a flat strip shunt would satisfy requirement (1) (stated above), but that the tubular design would be preferable.

As indicated above, the readily available theoretical formulas are not capable of yielding the effective 4-terminal impedance of a strip or tubular shunt at frequencies of 1 megacycle or higher. Due to the axial symmetry of the tubular shunt, it is possible to develop a theoretical formula for calculating the impedance of such a shunt, taking into account the nonuniform distribution of current over the thickness of the tube (skin effect), which will hold for very high frequencies. The development of this theoretical formula (taken from hitherto unpublished notes of F. B. Silsbee) is given in appendix 1, and it permits the impedance of any tubular shunt to be computed for frequencies up to 10^9 or higher. The development of a similar formula for strip shunts would be much more difficult because of the lack of axial symmetry.

The inductive effects of current-carrying parts other than the shunt upon the potential lead circuit of the shunt (requirement 2), are dependent upon two factors: (a) the mutual inductance of the current carrying parts upon any loop in the potential circuit of the shunt, and (b) the maximum rate of change of current with time in the current-carrying part.

The maximum rate of change of current occurs on the front of the current wave, and it is some-

[2] See p. 400 of reference [4] for inductance of tubular shunt.

[3] See p. 81 of reference [5] for inductance of a flat-strip shunt; p. 86 for skin effect of flat strip, and p. 91 for skin effect of a tubular shunt.

[4] See p. 81 of reference [5].

[5] See reference [5], p. 86 and 87.

times taken to be the peak value of current divided by the time to peak. This is actually the average rate of change for the front of the wave, and any detailed study of the front of a current surge requires a more accurate basis for obtaining the maximum rate of change of current. Theoretically, the maximum rate of change of current for a capacitance discharging through an inductance and resistance occurs at the instant the circuit is closed and is equal to the voltage, E, to which the condenser was charged divided by the inductance, L, in the discharge circuit. The total inductance of the discharge circuit of a surge-current generator can be as low as 2 μh, and with a maximum voltage of 100 kv the maximum rate of change of current would be 5×10^{10} amp per second. Such a rate of change of current in the main current circuit would induce 50 v in the potential circuit of the shunt if the mutual inductance, M, between the two circuits were 0.001 μh. As a "pick-up loop" in the potential lead circuit of only 1 sq cm area, placed very close to a current-carrying part, may have a mutual inductance of 0.002 μh (giving a peak induced voltage of 100 v), the extreme importance of minimizing mutual inductance between the potential circuit of a shunt and all current-carrying parts becomes apparent. If the surge generator discharge circuit is fairly long so that its total inductance is more than 2 μh, the maximum rate of change of current will not be correspondingly reduced, because the stray capacitance across the discharge circuit will in effect short out the added inductance at the instant the surge is being initiated.

Referring to figure 1, a, the potential circuit of a tubular shunt may be considered as an extension of the coaxial cable from the CRO, ending in a direct short circuit from the central conductor to the sheath. Due to the axial symmetry of this arrangement the mutual inductance between the potential circuit and any current-carrying parts is the lowest obtainable. Even when the sheath of the cable is connected to ground and ground currents flow in the sheath of the cable and in the outer current return tube of the shunt itself, these ground currents will not induce voltage in the potential circuit of the shunt provided the density of such currents is symmetrical around the axis of the shunt. End effects or concentration of current along one side of the shunt axis can be largely eliminated by extending the two current-carrying tubes of the shunt several diameters beyond the end of the central conductor that serves as a potential lead.

To reduce mutual inductance in the potential circuit of a strip shunt the potential leads can be taken off the strip as a central conductor and coaxial tube as shown in figure 1, b. There still remains the small loop formed by the resistance ribbon itself which is in the potential circuit of the shunt and offers the possibility of inductive pick-up from such currents as might flow in the sheath of the cable and one of the current leads up to the potential circuit. There is no way of separating the potential circuit from end effects arising from such currents in a strip shunt. Although a strip shunt could be built with very low inductive pick-up between its potential circuit and current-carrying parts, the tubular shunt is the only design offering the possibility of entirely eliminating such inductive effects.

In order to understand the importance of being able to ground the sheath of the cable going from the shunt to the CRO at or near the shunt (requirement (3) above), it is necessary to consider the entire surge-current generator circuit. A schematic diagram of a surge-current generator is given in figure 2. The heavy lines show the path of the surge current from capacitor, C, through the tripping gap, test specimen, measuring shunt and the necessary connecting leads. No ground connections are necessary to complete the heavy-current discharge circuit, but this circuit is usually tied to the ground or the floor of the laboratory at some point between the low-voltage terminal of the capacitors and the test specimen in order to complete the charging circuit and to definitely fix the potentials of various parts of the discharge circuit with respect to ground. The self-inductance of the conductors forming the discharge circuit will depend upon their cross-section, length, and arrangement. Assuming the conductors to be of round cross section ½ in. in diameter, their inductance is 0.01 μ h per cm length for a return at a considerable distance. For the maximum rate of change of current 5×10^{10} amp per second, this means the maximum voltage difference between two points 1 cm apart on this discharge circuit is 500 v. Thus, if the discharge circuit were grounded at point g in figure 2, a shunt located only 10 cm from point g would be 5,000 v above ground as the discharge is initiated. This voltage will tend to

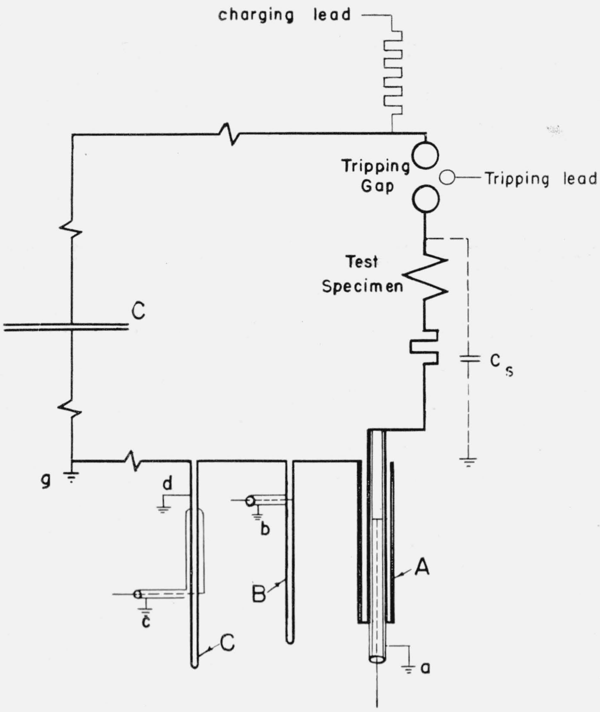

FIGURE 2. *Wiring diagram of surge-current generator showing method of connecting shunts, their potential lead arrangement, and several possible ground connections.*

make current flow in the sheath of the cable from the shunt to the CRO, through the ground connection at the CRO and back to point *g* through the laboratory grounding system. Due to the stray capacitance (C_s in fig. 2) from the lower ball of the tripping gap and parts of the discharge circuit to ground, this voltage will be of a high frequency oscillatory type occurring just as the main current discharge is initiated and any currents caused by it will induce voltages of the same character in any circuit coupled with them. In order to minimize such inductive effects at the CRO it is necessary that the cable from the shunt to the CRO have its sheath grounded at or near the shunt. In order to reduce the effect of stray capacitance (C_s in fig. 2) it may be desirable to ground other points in the discharge circuit, such as *g*, in addition to the sheath of the cable. Thus, the best type of shunt would be one which would allow any or all of these ground connections to be made and still have minimum pick-up due to induced voltages from ground currents.

In figure 2, all of the three types of shunts illustrated in figure 1 are represented as being connected in the discharge circuit of a surge generator in order to help explain the effect of ground currents on each. The ground currents most likely to cause inductive pick-up are those due to the high frequency oscillations arising from the stray capacitance, C_s, to ground. If a type *C* strip shunt were used, a consideration of the various possible ground connections in addition to the cable sheath ground at the CRO, leads to the following conclusions: (1) a single additional ground connection to the cable sheath at *c* would not be suitable, because then ground currents from C_s would flow in one potential lead of the shunt and induce high voltages in the loop formed by the potential leads; (2) a single additional ground connection at *g* would still permit cable-sheath currents, which flow to ground at the CRO end of the cable, to flow through one of the shunt potential leads (actually this is better than no ground at *g*); (3) two additional grounds, one at *g* and one at *c* would introduce a combination of the two above effects without eliminating either; (4) a single additional ground at *d* would reduce the inductive effects of ground currents but would not eliminate them entirely.

Thus the use of a shunt of this type would preclude the experimentally desirable flexibility in location of ground connections.

If a type *B* strip shunt were used, the same conclusions given for the type *C* would hold except all inductive effects would be much less because, as may be seen from the diagram, the arrangement of potential leads insures a lower mutual inductance between the potential circuit and current-carrying parts.

If a tubular, type *A*, shunt were used the ground current for any combination of ground connections would be symmetrically distributed around the axis of the coaxial potential circuit, thus, theoretically at least, eliminating any pick-up due to these ground currents.

The above considerations indicate that the coaxial tubular design is superior to other designs in surge-current measurement work because (1) it should be more constant in impedance over a wide range in frequency, (2) it can be constructed to insure minimum inductive pick-up from current-carrying parts of the surge generator, and (3) it offers the greatest freedom in location of ground connections at the surge generator. In view of these advantages it was decided to investigate theoretically as well as experimentally the advantages and limitations of concentric tubular shunts for surge current measurements, realizing that some of the derived relations would be applicable to strip-type shunts.

2. Determination of Cross-Sectional Area and Length

The cross-sectional area and length of a shunt are related as follows:

$$V=lA$$
$$R=\rho l/A$$

where V is the volume of the resistance material, l its effective length, A the cross-sectional area, R the resistance, and ρ the volume resistivity.

Solving for A and l

$$A=\sqrt{\frac{V\rho}{R}} \qquad (1)$$

$$l=\sqrt{\frac{VR}{\rho}} \qquad (2)$$

The resistivity, ρ, is a constant of the shunt material, and it is well to choose a material having as high a resistivity as possible. The resistance of the shunt is determined by the maximum current to be measured and the maximum voltage that can be recorded at the CRO. The volume of the shunt resistance material is fixed by the largest amount of energy that must be absorbed by it during a single discharge of the surge generator. A reasonable temperature rise of say 100° C allows a thermal input of 100 times the specific heat times the mass of the shunt material. For most metals the specific heat is about 0.1 and density is 9, so in general the maximum allowable thermal input to the shunt would be 90 times V, in calories for V in cubic centimeters. The maximum energy fed into the shunt during a single discharge is equal to the energy initially stored in the surge generator capacitors ($1/2\ C\ E^2$), times the resistance of the shunt divided by the minimum effective resistance of the surge-generator circuit. As this minimum effective resistance is usually at least twice that of the shunt, the maximum shunt input energy may be taken as $1/4\ C\ E^2$. When the volume of shunt material computed from this energy input is inserted in the above equations, approximate values of l and A for the shunt are determined. It is best to choose the thinnest wall tubing available having approximately this cross-sectional area as the thinner the wall the slower the change in effective impedance as the frequency is increased (see appendix 1). The limit on wall thinness is set by magnetic stresses, to be discussed later.

If for practical reasons the values actually chosen for l and A differ markedly from the approximate values computed from eq 1 and 2 (this will necessarily be true if the preliminary value of l is too long for convenience or if tubing having approximately the estimated cross-sectional area is not available) the allowable energy input should be computed for the chosen values. This allowable energy input together with the resistance of the shunt and the maximum energy available from the surge generator ($\frac{1}{2}\ CE^2$) determine a minimum effective resistance for the surge-generator discharge circuit. Except in cases where an oscillatory discharge with extremely low damping is required, this minimum effective resistance will be exceeded.

3. Forces on a Tubular Shunt

When a heavy surge current is passed through a tube made of resistance material, it will be subjected to forces from two sources: (1) the action of the magnetic field produced by the current upon the current itself and (2) the thermal expansion of the tube arising from its sudden change in temperature when the current is applied. The magnetic force acts as a pressure from the outside tending to collapse the tube. A formula for computing this pressure is derived in appendix 2. It depends upon the square of the current through the tube and upon its cross-sectional dimensions. Except for extremely high currents most thin-wall tubes available for use in a shunt would probably withstand the pressure arising from the magnetic field; however, in the design of any shunt, and especially in the case of a shunt made with extra-thin-wall tubing, this pressure should be computed in order to make sure that the tube will not collapse.

The sudden change in shunt temperature when the discharge occurs introduces a stress in the tube whose approximate value can be computed. As the shunt tube itself is made of material having much higher resistivity than other current-carrying parts of the shunt and surge generator circuit, it will momentarily attain a higher temperature than its supporting parts during each current discharge. This sudden change in temperature tends to increase the length of the tube, but it occurs so fast the tube does not have time to expand, and the tube is momentarily put in compression. The maximum compressive stress may be computed from the strain (total temperature change T, times coefficient of linear expansion, δ) and the stress-strain curve for the shunt material. The tube will then behave somewhat like a spring initially compressed and suddenly released; i. e., waves of stress will proceed along the tube, with the velocity of sound, being reflected at the ends and traveling back as tensile stress. The nature and magnitude of these stresses could be computed for any given tube if the exact masses connected to the two ends of the tube were known; however, the maximum stress would not be expected to greatly exceed the initial compressive stress that may easily be computed as noted above. Assuming the shunt material to be perfectly elastic and that it will not be stressed beyond its elastic limit, the maximum stress will be

$$S = ET\delta, \tag{3}$$

where E is the modulus of elasticity for the shunt material. If a value for S is taken equal to the maximum allowable stress (just below yield point) for the material being used, this equation gives an allowable temperature rise for the shunt. For most materials this allowable temperature rise is about 100° C. This value could probably be exceeded because of the high ductility of most resistance alloys; thus if a minimum resistance is desired in the surge generator discharge circuit (maximum energy in the shunt) it would be advisable to determine the maximum allowable temperature rise or energy input experimentally.

This could be done by placing a sample of tubing of the same material and cross-sectional dimensions as the shunt tube in the discharge circuit of a surge-current generator. The energy absorbed by the sample may be computed by multiplying the energy initially stored in the capacitors ($\frac{1}{2}CE^2$) by the ratio of the resistance of the sample to the total effective resistance of the complete surge generator discharge circuit including the sample tube. The total effective resistance of the surge generator can be deduced by using a shunt, whose resistance tube has a cross-sectional area at least five times that of the sample tube, in the discharge circuit and taking oscillograms of the discharge current. From measurements of frequency and logarithmic decrement on these oscillograms, the inductance and effective resistance of the complete surge-generator discharge circuit can be computed. Thus, by starting with the surge generator capacitors charged to a fairly low voltage, E, and taking repeated discharges through the sample tube at successively higher values of E the energy input at which the tube is broken or deformed may be determined. The safe allowable temperature rise for a tube of this particular material and size can then be stated.

The experimental procedure just described was carried out for a 5/16-in. diameter CuNi alloy tube whose wall thickness was 0.039 cm and length 33 cm. No evidence of tube failure except discoloration due to the high temperature was noted for energy inputs below 160 joules/centimeter (instantaneous temperature rise of 400° C). However, after the first discharge at this energy input a slight bend in the tube was noted as though it were failing as a column in compression. After each discharge of successively higher energy input the bending was more pronounced and after a discharge at 268 j/cm (670° C temperature rise) in addition to the bending, decided crinkling and crushing were noted. The crushing was probably caused by magnetic forces acting at an instant when the tube was weakened because of its high temperature. These values of energy input exceed what might be considered a desirable design value.

The safe design value should be one that would not stress the tube beyond its elastic limit. This was determined in another experiment by measuring the length of the tube before and after each discharge. After two discharges, the energy input of each being equal to 60 j/cm (150° C temperature rise), no permanent change in length was noted. For energy inputs of 100 j/cm (260° C temperature rise) or greater an increase in length of about 0.2 mm (0.6 percent) was noted after each discharge. Thus, it was concluded that the maximum allowable temperature rise for a shunt made of this material should be about 150° C. This is only slightly above the maximum value (133° C) computed from the stress due to thermal expansion.

4. Inductance and Capacitance Between Current Terminals

Because of the method of attaching potential leads, the 4-terminal impedance of a tubular shunt is constant over a wide range of frequency. However, at very high rates of change of current (high-frequency components of the surge), the distributed capacitance and inductance of the current circuit will cause variations in the root-mean-square values of these high-frequency components along the length of the shunt. That is, the instantaneous value of current along the length may differ from the value at the current terminals.

This variation in the instantaneous value of current along the length of the shunt is, of course, entirely negligible at lower frequencies, but in order to determine the frequency at which this effect becomes appreciable a solution for the current and voltage along the length of the tube, assuming uniformly distributed inductance and capacitance only, was obtained (in a manner similar to that used in appendices 3 and 4). The current at the potential lead end of the shunt, I_l, was found to be

$$I_l = \frac{I_c}{\cos \omega l \sqrt{LC}} \tag{4}$$

where

I_c=current at current terminals; L=distributed inductance per unit length of shunt; C=distributed capacitance per unit length of shunt; $\omega = 2\pi f$ (f in cycles per second); l=length of current circuit in centimeters.

For concentric tubes whose wall thickness is small compared to their diameter, the inductance and capacitance per unit length are:

$$L = 2 \log_\epsilon b/a \times 10^{-9} \text{ henries} \tag{5}$$

and

$$C = \frac{0.555}{\log_\epsilon b/a} \times 10^{-12} \text{ farads} \tag{6}$$

where a is the outer diameter of the inner tube, and b is the inner diameter of the outer tube. Multiplying eq 5 by eq 6 gives $LC = 1.110 \times 10^{-21}$. Thus the quantity $\sqrt{LC}$ in eq 4 is a constant, and the variation in current along the length of the tubes depends only upon the length, l, of the tubes and the frequency of the current being measured. For shunts up to 100 cm long, the maximum variation in current is less than 10 percent for frequencies up to 21.5 megacycles.

The voltage between the current terminals was found to be

$$E_0 = j\omega L l I \left(1 + \frac{\omega^2 LC}{3} l^2 + \ldots\right) \tag{7}$$

The magnitude of this voltage does not affect the accuracy of the shunt, but it should be evaluated to indicate the insulation required between current terminals. For shunts up to 100 cm long the quantity in the bracket of eq 7 reduces to unity (within 5 percent) for frequencies up to 18 megacycles. Thus this voltage may be taken as equal to $j\omega L l I$ or $L l dI/dt$. The total inductance of the current circuit for any tubular shunt, Ll, may be computed from its dimensions by use of eq 5, and the rate of change of current dI/dt depends upon the particular surge generator being used and its discharge circuit. For a typical shunt, 100 cm long, this inductance is about 0.14×10^{-6} henries, and for the maximum rate of change of current assumed above (5×10^{10} amp/sec) the voltage between current terminals is 7,000 v.

III. Description of Two Shunts

There are two surge generators being used in this laboratory at the present time. One is a 2,000 kv surge-voltage generator capable of giving 30,000 amp on short circuit. The other is a 100 kv 10μf surge-current generator capable of discharging a maximum of 200,000 amp. It was

TABLE 1.—*Constants of two tubular shunts*

	Shunt A	Shunt B
Four-terminal resistance	0.04 ohm	0.0048 ohm
Over-all length	39 in	38¼ in.
Length of resistance tube	26 7/16 in	24 7/16 in.
Diameter of outside tube	⅞ in	2 in.
Diameter of resistance tube	¼ in	1 in.
Wall thickness of resistance tube	0.008 in. (0.0203 cm).	0.0246 in. (0.06 cm).
Cross-sectional area of resistance tube	0.0392 sq cm	0.469 sq cm
Resistance tube material	German silver	80% Cu, 20% Ni
Resistivity of resistance tube (micro-ohm cm).	23.33	36.3
Ratio of a-c impedance to d-c resistance, at:		
f=0.25 megacycle	1.00	0.98
f=0.50 megacycle	1.00	0.92
f=1.0 megacycles	0.99	0.76
f=2.0 megacycles	0.96	0.48
f=5.0 megacycles	0.86	0.15
Allowable temperature rise—computed from stress due to thermal expansion	133°C	133°C
Allowable energy input	1320 joules	14,500 joules
Current limit due to magnetic force	87,600 amp	223,000 amp
Total inductance of current circuit	0.202 μh	0.106 μh
Maximum voltage drop at current terminals—$L\, di/dt$ for $di/dt = 5 \times 10^{10}$ amp/sec	10,000 v	5,300 v

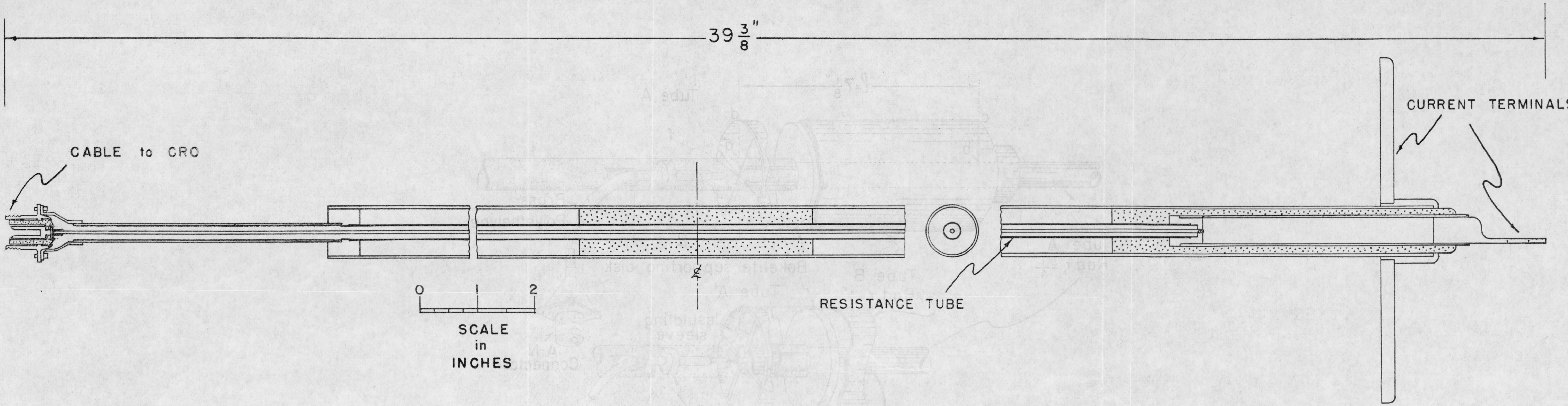

FIGURE 3.—*Structural details of small tubular shunt, A.*
See table 1 for additional dimensions and other constants.

FIGURE 4.—*Structural details of large tubular shunt, B.*
See table 1 for additional dimensions and other constants.

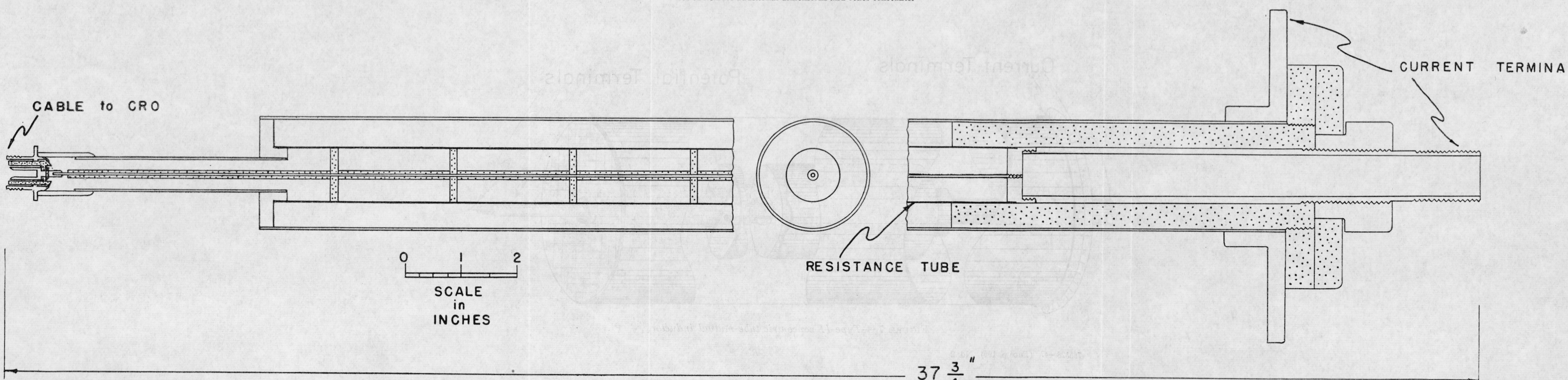

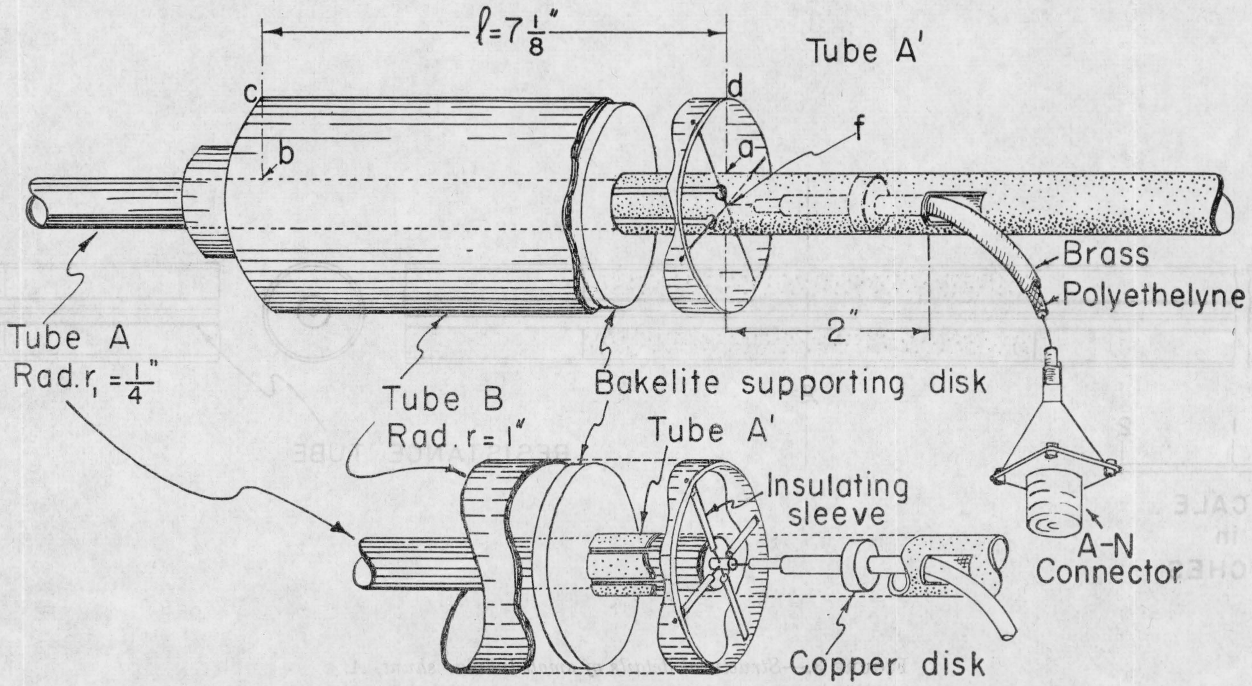

FIGURE 6.—*Type I concentric tube mutual inductor.*

M=0.05 μh.

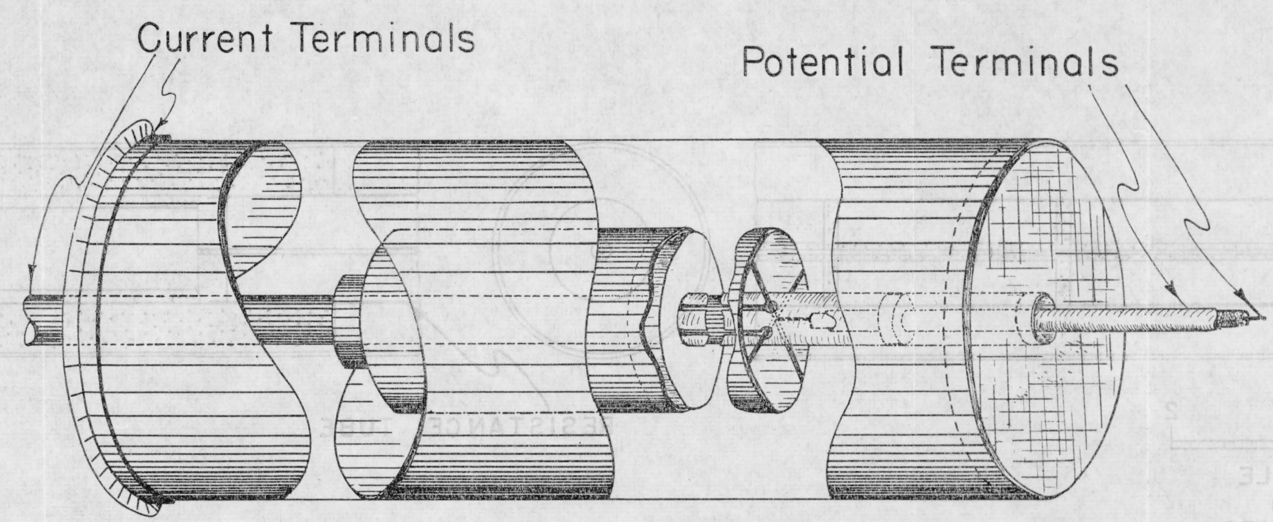

FIGURE 7.—*Type II concentric tube mutual inductor.*

thought that at least two shunts would be needed, one for currents from 10,000 to 50,000 amp and one for currents from 50,000 to 200,000 amp. As the CRO was capable of giving satisfactory records over the range from 200 to 2,000 v when used with a suitable potential divider at the deflecting plates, resistance values of 0.04 and 0.005 ohm were chosen for the two shunts that have been constructed. Cross-sectional drawings of the shunts are shown in figures 3 and 4. Their physical and computed constants are given in table 1. The resistance tubes were selected from a small stock of readily available thin-wall tubes, because at the time it was not feasible to wait for special tubes to be drawn.

The ratios of *a-c* impedance to *d-c* resistance given in table 1 were computed from the theoretical formulae derived in appendix 1. At frequencies above 5 megacycles for the 0.04 ohm and 1 megacycle for the 0.0048 ohm shunt, this ratio is considerably less than unity. This fact is of no great concern in the measurement of the present standard impulse-current test waves for which the fundamental-frequency component is of the order of 100 kc or less; but the fact should not be overlooked that the magnitude of higher-frequency components, probably present in such test waves, may be considerably reduced on a comparative basis. Other types of shunts, as they have some inductive coupling between their potential-lead circuit and current-carrying parts of the discharge circuit, may give an indication of these higher frequency superposed currents. However, this indication will depend, not upon the resistance of the shunt, but upon the unknown value of inductive coupling, and thus will give an erroneous idea of their magnitude. A method of accurately determining the magnitude of high-frequency components consists of using a mutual inductor, having a known value of coupling with the current circuit, in place of a shunt. Mutual inductors have been constructed and are used at this laboratory. They will be discussed in section IV.

The allowable energy input for these shunts was computed from the allowable temperature rise (obtained from the maximum stress due to thermal expansion) and the mass of each shunt (actual values are given in table 1). These values are useful in computing the minimum resistance that can be used in the discharge circuit of a surge generator without overheating these shunts. As an example: The surge voltage generator in this laboratory requires the dissipation of 33,300 j for each discharge when charged to full-rated voltage. Thus, when shunt A is used with this generator, the total resistance of the discharge circuit must be at least 33,300 divided by 1,320 times the shunt resistance (0.04 ohm) or 1.01 ohms. A similar computation for shunt B gives 0.107 ohm. As the minimum discharge resistance of this surge voltage generator is 6 ohms, either shunt may be used with any discharge circuit. The surge-current generator in this laboratory requires the dissipation of 50,000 joules when charged to full-rated voltage, thus the total resistance of the discharge circuit must be at least 1.52 ohms if shunt A is to be used or 0.0165 ohm if shunt B is to be used. As the minimum discharge resistance of this surge-current generator is 0.03 ohm, shunt B may be used with any discharge circuit, but shunt A should only be used when a resistance of at least 1.5 ohms is added (a resistance of about this value is needed to give a critically damped discharge).

The current limitations on these shunts due to magnetic forces were estimated by the formula given in appendix 2. These limitations are above the values of current expected to be used with these shunts. The inductances of the current circuits of these shunts were computed by using the formula given in eq. 5. The voltage drops computed from these inductances and the maximum expected rate of change of current indicate the desirability of having adequate insulation between the current terminals to prevent flashover.

IV. Mutual Inductors for Measuring Rates of Change of Current

1. General Considerations

For many experiments involving heavy-current surges, it is desirable to know the wave form of the rate of change of current, for example: (1) in studying the voltage induced in a circuit coupled with the heavy current discharge circuit and (2) in studying the voltage difference arising from inductance between two points on a conductor or a system of conductors carrying the heavy-surge current. The rate of change of current can be computed from an oscillogram of the current obtained by using a shunt, but this involves the inaccuracy of measuring the slope of the current wave at a number of points and plotting a curve from these measured values of slope. In addition, the high-frequency components of the current wave form as they appear in the oscillogram obtained with a shunt may be highly distorted or attenuated and give an erroneous value of rate of change of current, especially at the point of maximum rate of change. A more accurate record of rate of change of current can be obtained with much less effort by inserting the primary of a mutual inductor in the heavy-current discharge circuit in place of the shunt and connecting the secondary of this inductor to the cable to the CRO. The record obtained on the CRO is then equal to $M\ di/dt$. If M (the mutual inductance of the inductor) is known, an actual oscillogram of the rate of change of current is obtained.

A mutual inductor, to be considered satisfactory for this purpose, must fulfill the following requirements: (1) Its mutual inductance must be of suitable value to give the proper voltage at the CRO (from 500 to 2,000 in this case). For the expected rates of change of current (from 1 to 5 times 10^{10} amp per second) this amounts to about 0.05 μh. This value of mutual inductance must be definite and should be computable from the physical dimensions of the inductor.

(2) The primary circuit of the inductor must be capable of carrying the heavy current discharge and should add a minimum impedance to the discharge circuit.

(3) The secondary circuit should have minimum coupling to all current carrying parts except the primary of the inductor.

(4) The method of connecting the secondary circuit to the cable going to the CRO should be such that the sheath of this cable can be connected to ground near the surge current generator without introducing coupling between ground currents in the sheath and the secondary circuit.

(5) The secondary circuit should have a minimum self-inductance. This may be explained as follows: The voltage to be measured at the CRO ($M\ dI/dt$) is impressed upon a circuit containing the self-inductance, L, of the secondary circuit and the surge impedance, R, of the cable to the CRO. It is the voltage across the surge impedance, R, that is recorded at the CRO and its value is

$$E_{\text{CRO}}=\frac{M\ dI/dt}{1+j\frac{\omega L}{R}}. \qquad (8)$$

In order to have E_{CRO} equal to $M\ dI/dt$ for the high frequency components of I, it is apparent that the self-inductance, L, of the mutual inductor secondary circuit should be kept as low as possible. As L cannot be reduced to zero, the highest frequency components of I are subject to a phase displacement and attenuation, the magnitudes of which can be computed from the above equation for any assumed value of $\omega=(2\pi f)$.

A consideration of the various convention types of mutual inductors leads to the conclusion that none of them will fulfill the above requirements satisfactorily. The most promising type appeared to be one consisting of a straight single conductor primary insulated from, and running through, the central axis of a toroidal coil secondary of sufficient turns to provide adequate voltage at the CRO. It was thought that by introducing shields and connecting them to the primary circuit at an appropriate point with respect to the ground connection, an inductor of this type might fulfill most of the requirements listed above. A preliminary design of an inductor of this type was carried out, but the self-inductance of its secondary circuit had to be at least 2 μh in order to give the desired value of mutual inductance. When this value of inductance and 50 ohms for the CRO cable surge impedance, R, are inserted in eq. 8, it is found that the voltage at the CRO is only 0.9 of $M\frac{dI}{dt}$ for a frequency of 1.8 megacycles, for higher frequencies the attenuation would be much greater. The use of a mutual inductor of this type was, therefore, abandoned.

2. Mutual Inductors of Special Design

The first attempt to design a special mutual inductor to meet all of the requirements listed above resulted in the inductor shown in figure 5. The primary circuit is the straight length of No. 10 copper wire (with the return circuit at least 2 ft away, its effect can be neglected). The secondary circuit consists of the "D" formed by part of the No. 10 wire and the No. 16 wire. This arrangement permits the magnetic flux linking the secondary "D" to be computed as that due to an infinitely long, straight conductor, neglecting the effect of the return lead. The self-inductance of the secondary circuit is that due to the single "D" loop and can also be computed from its dimensions.

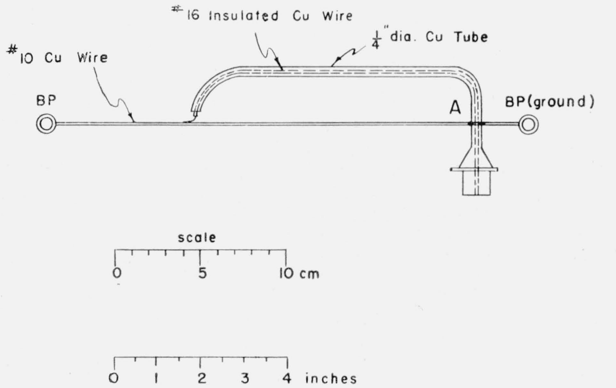

FIGURE 5.—*D-type mutual inductor used to obtain records of rate of change of surge currents.*

M=0.0986 μh

An inductor of this design, with dimensions corresponding to the scale in figure 5 was constructed. Its mutual inductance was computed to be 0.0986 μh and the self-inductance of its secondary circuit 0.25 μh. This value of self-inductance is considerably less than that of the toroidal secondary circuit mentioned earlier, and as a consequence frequencies up to 15 megacycles will be recorded with only 10 percent reduction in magnitude. The secondary circuit is connected to the CRO cable by coaxial leads, thus no voltage will be induced in it from ground currents flowing in the cable sheath. A mutual inductor of this type appears to fulfill the requirements of surge current testing fairly well. The one constructed in this laboratory has been of considerable value in obtaining records of the rate of change of surge currents. Its outstanding advantage lies in simplicity of construction.

The "D"-type mutual inductor has some drawbacks: (1) it is not completely unaffected by magnetic fields produced by other current-carrying parts of the surge generator circuit and (2) the self-inductance of its secondary circuit is about three times its mutual inductance (as a minimum it should be possible to make an inductor whose self-inductance is as low as its mutual inductance). Another mutual inductor has been designed in which the secondary circuit consists of a tube arranged coaxially with the primary conductor in order to overcome the small defects inherent in the "D"-type inductor.

A type I coaxial tube mutual inductor is shown in figure 6. Tube A constitutes the primary circuit of this inductor (the surge-current return lead is again assumed to be located at least 24 in. away so its effect can be neglected). The secondary circuit of this inductor consists of the following parts: (1) tube, A, from a to b, (2) a radial ring soldered on its inside to and around tube A at b and soldered on its outside to and around the inside of tube, B, at c, (3) tube B from c to d, and (4) the four-wire radial "spider" connection from d on tube B, going through but insulated from tube, A, and soldered to the central conductor of the potential leads at f. The secondary terminals are thus at a and f and are brought out through the concentric leads to the fitting for the CRO cable. How well this design of mutual inductor fulfills each of the requirements listed above may best be seen by considering each requirement, as follows: (1) The mutual inductance can be computed as that due to the magnetic flux produced by current in a long straight conductor (tube A) integrated over the region $a\ b\ c\ d\ a$ between the tubes. The mutual inductance thus derived in terms of the tube dimensions indicated on figure 6 is

$$M=2l \log_\epsilon \frac{r_2}{r_1}\, 10^{-9} \text{ henry (for } l \text{ in cm).}$$

There is a small correction to this value of inductance due to the thickness of tubes A and B, which can be computed by the method explained on page 397 of reference [4]. For $r_1=0.25$ in. and $r_2=1$ in., the length, l, of tube B should be about 7 in. to give a mutual inductance of 0.05 μh. (2) Because of the method of bringing out the secondary circuit leads used in this design, tube A must be at least 0.5 in. in diameter, and it should be made of a good conducting material such as copper. The wall thickness of this tube is relatively unimportant, and any ordinary thin wall copper tube can be used that is adequate to carry the heavy current discharge without damage. (3) The secondary circuit except for the ring and spider are coaxial conductors and thus have minimum coupling to all currents not flowing in the inductor. Likewise the radial ring and spider conductors are symmetrical about the axis which results in minimum coupling. (4) Also, because of the coaxial arrangement of the secondary circuit and leads to the CRO cable, any ground currents flowing in the cable sheath will have minimum coupling with the secondary circuit and leads. (5) The self-inductance of the secondary circuit can be computed by the method explained on page 397 of reference [4], and it is found to be equal to the mutual inductance except for a small term arising from the finite thickness of tube, B. The self-inductance of the spider alone is less than 0.005 μh. Thus this design gives the minimum self-inductance that can be obtained in a straightforward manner.

An approximate value of the voltage impressed on the CRO cable can be obtained from eq. 8, but this equation neglects the capacitance between tube, A, and tube, B, and will not hold for the higher frequencies. A more accurate method for computing the value of this voltage is to consider the capacitance and inductance of the secondary circuit to be uniformly distributed along its length and solve for the voltage at the CRO end of this circuit by the methods normally used for circuits of uniformly distributed constants. This is done in appendix 3, and as shown there for a typical mutual inductor designed for surge-current measurements, the voltage impressed on the CRO cable will be equal to $M\, dI/dt$ (within 10 percent) for all frequencies up to 65 megacycles/sec.

The type I tubular mutual inductor appears to satisfy the requirements for surge-current measurement quite well. One was constructed in this laboratory having the approximate dimensions indicated in figure 6. This type of inductor is entirely satisfactory if the surge-generator discharge circuit is fairly long and can be arranged so that the inductor forms the final part of the return lead to ground. In case the minimum length of discharge circuit is required, the length of this inductor may add an appreciable inductance to the discharge circuit and it may also not be feasible to keep the return lead 24 in. away from the axis of the inductor. For such cases, a slightly different design of tubular inductor (type II) as indicated in figure 7 is suggested. It is the same as the type I inductor except that a return circuit is provided for the current by a larger tube, coaxial with the smaller tubes. This design brings the two current terminals close together and eliminates the problem of the location of the inductor with respect to other parts of the surge-generator circuit. It allows the inductor to be used in a discharge circuit of minimum length with the addition of the least possible inductance to the discharge circuit. The outer current return tube of the type II inductor also acts as an electrostatic shield for its secondary circuit. Because of the distributed capacitance between the outer-current return tube and the coaxial secondary circuit tube, currents and voltages in the secondary circuit will not be the same for the type II inductor as for the type I. Thus a computation of the voltage impressed on the CRO cable for a type II inductor must take into account the distributed capacitance and inductance of the circuit formed by the outer tube of the secondary circuit and the return current tube in addition to that of the secondary circuit itself. This is done in appendix 4, and while the results appear quite different from those obtained for the type I inductor in appendix 3, they indicate about the same upper limit in frequency (70 megacycles/sec).

Each of the three types of mutual inductors described above should prove useful for surge-current measurements. The "D" mutual inductor is very simple to construct and will measure superposed frequencies up to 15 megacycles/sec with less than 10 percent error. The tubular inductors are somewhat more complicated to construct but extend the frequency range to 70 megacycles/sec. The type I tubular inductor is suitable when the surge-generator discharge path is fairly long and the type II when a minimum length of discharge path is required. Inductors of both the "D"-type and the type I tubular have been constructed and proved very useful in this laboratory.

V. Experimental Results

The shunts and mutual inductors described above have been used in this laboratory for measuring current surges both from a surge-voltage generator and a surge-current generator and for various arrangements of discharge circuits. The oscillograms in figure 8 are typical of the results obtained. They are records of the discharge current and rate of change of current for a surge-current generator consisting of 40 1-μf, 50-kv, capacitors connected in series-parallel so as to give a total capacitance of 10 μf and a voltage rating of 100 kv. The discharge circuit consisted of a

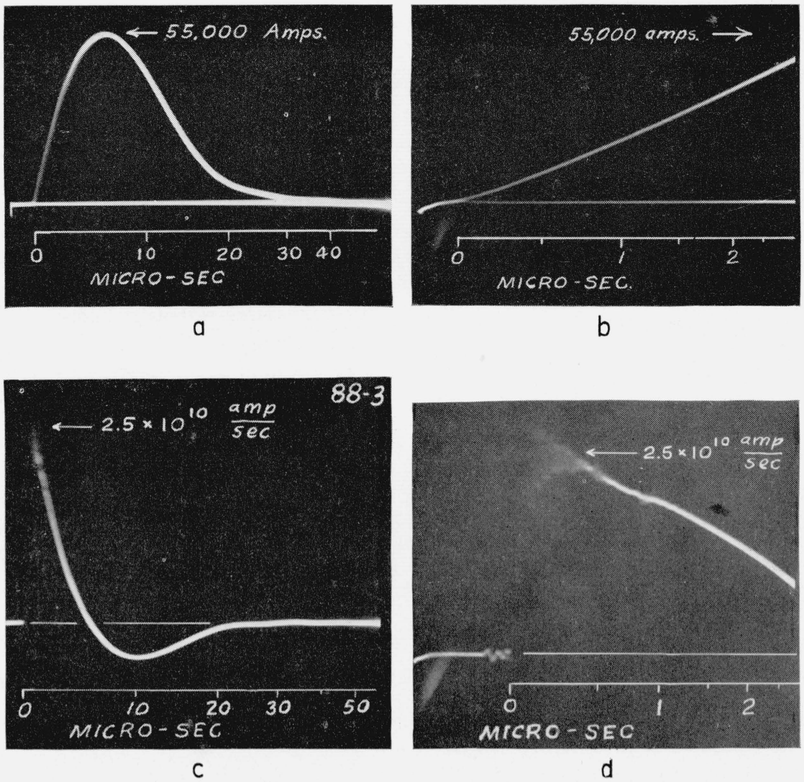

FIGURE 8.—CRO *records of a critically damped discharge from a surge-current generator.*

a, Current wave-form obtained by use of tubular shunt, *A*. *b*, early part of current wave-form on a faster CRO sweep. *c*, rate of change of current obtained by use of the mutual inductor shown in figure 6; *d*, early part of rate of change on a faster CRO sweep.

three-ball triggering gap; a 1-ohm resistor made up of 24 globar type B ceramic resistor units, assembled in the form of a cage (to minimize inductance) having sets of two 12-in. units in series, connected in parallel so that this assembly was 24 in. long; about 5 ft of copper busbar; and the shunt or mutual inductor. The total inductance of this generator and its discharge circuit is 2.5 μh and the 1-ohm resistor gives very close to critical damping. For the oscillograms shown in figure 8 the generator was charged to 75 kv and gave a maximum discharge current of 55,000 amp, the maximum rate of change of current being 2.5×10^{10} amp/sec

The oscillogram in figure 8, a, shows the variation of current with time for the entire surge. Figure 8, b, shows the initial rise of the current on an expanded time scale (faster CRO sweep). Figure 8, c, shows the variation in the rate of change of current for the entire surge, and figure 8, d, shows the initial rate of change of current using a faster sweep. The current records are quite smooth and just as anticipated from theory, as are the rate of change of current records except for the superposed high-frequency oscillations occurring just as the surge is initiated. These superposed oscillations have a frequency of about 40 megacycles and are probably caused by stray capacitance across parts of the discharge circuit, such as from one ball of the tripping gap to ground. If this stray capacitance is across a section of the discharge circuit having an inductance of 2 μh, it would require only about 10 $\mu\mu$f to produce the 40 megacycle oscillations. It is practically impossible to eliminate such stray capacitances. In the discharge circuit used in obtaining the oscillograms of figure 8, stray capacitances were reduced to as low a value as possible. For discharge circuits involving fairly large apparatus as a test specimen, stray capacitances will be larger, resulting in a superposed oscillation of lower frequency.

The slight upward curvature on the zero line of oscillograms in figures 8, b and 8, d at the start of the sweep is introduced by the oscillograph and should not be considered as part of the surge record. The source of this "hook" in the CRO zero line is a small horizontal deflection given to the beam by the Norinder relay plates as voltage is initially applied to them. This deflection slightly alters the CRO sweep rate at its beginning but should, by itself, introduce no vertical deflection. However, since the focusing coil is located below the Norinder relay plates, this deflection puts the beam slightly off the axis of the focusing coil which then produces the small vertical deflection.

The oscillograms in figure 8 illustrate the advantages of using a mutual inductor in addition to a shunt when measurements of a current surge are being made. The superposed oscillations cannot be detected on the current record but can readily be seen and measured on the rate-of-change-of-current record. Their actual magnitudes in amperes can be computed from this record, and from measurements on the oscillogram of figure 8, d they were found to have a maximum amplitude of about 25 amp. Oscillations of this magnitude would be almost impossible to detect on a current record even though the attenuation of the shunt for these higher frequencies did not mask them out. The rate of change of current records are also of great value in studying the effects of induced voltages arising from the current surge. They further provide an accurate measurement for the time to maximum current (zero rate of change).

VI. References

[1] P. L. Bellaschi, Heavy surge currents—generation and measurement, Electrical Eng. **53,** 86 (Jan. 1934).

[2] T. Brownlee, Discussion of Bellaschi's paper, Heavy surge currents—generation and measurement, Electrical Eng. **53,** 481 (Mar. 1934).

[3] N. Rohats, A surge-current generator, General Electric Rev. **37,** 296 (June 1934).

[4] F. B. Silsbee, A study of the inductance of four-terminal resistance standards, Bul BS **13,** 375 (1916) S281.

[5] F. B. Silsbee, Notes on the design of four-terminal resistance standards for alternating current, BS J. Research **4,** 73 (1930). RP133.

VII. Appendices

1. Effective Impedance of a Tubular Shunt as a Function of Frequency [6]

Let the radii of the inner and outer tubes be a, b, a', and b' as indicated in figure 9. Assuming the tubes to be coaxial and perfectly symmetrical about their axis the current density in either tube at a given radius, r, from the axis will be a constant for any given instant, so let

i_r = current density in inner tube at radius r, + if into paper

i_r' = current density in outer tube at radius r, + if into paper

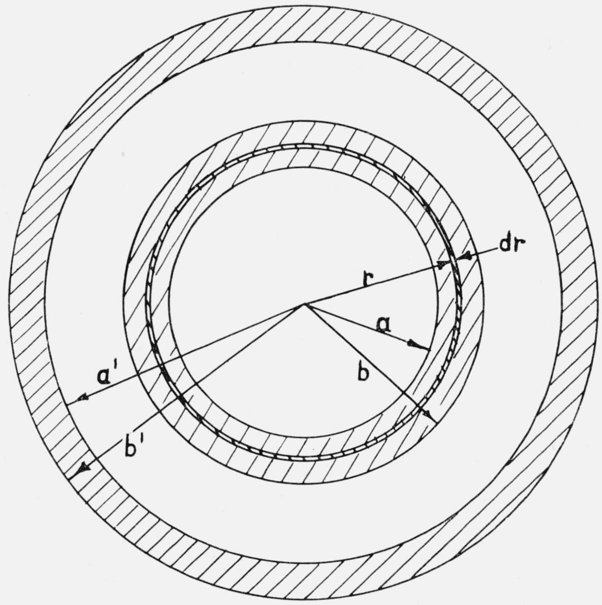

FIGURE 9.—*Cross-sectional view of a tubular shunt.*

Then

$$I = \text{total instaneous current in inner tube} = \int_b^a 2\pi i_r r dr$$

$$I' = \text{total instantaneous current in outer tube} = \int_{b'}^{a'} 2\pi i_r' r dr$$

Also, let:

e = emf drop per unit length of inner tube

e' = emf drop per unit length of outer tube

H_r = magnetic field at r taken + if clockwise

ρ = resistivity of inner tube material

ρ' = resistivity of outer tube material

Φ_r = total magnetic flux outside of radius r (all permeabilities assumed = 1).

NOTE.—The cgs magnetic system of units is used throughout this derivation and all dimensions are in centimeters.

[6] This derivation is taken from hitherto unpublished notes of F. B. Silsbee.

As all currents flow along lines parallel to the tube axis, e and e' are independent of r, so

$$e=\rho i_r+\frac{\partial\Phi_r}{\partial t} \tag{9}$$

$$e'=\rho' i_r'+\frac{\partial\Phi_r'}{\partial t} \tag{10}$$

and

$$\frac{\partial e}{\partial r}=\rho\frac{\partial i_r}{\partial r}+\frac{\partial}{\partial t}\frac{\partial\Phi_r}{\partial r}=0 \tag{11}$$

$$\frac{\partial e'}{\partial r}=\rho'\frac{\partial i_r'}{\partial r}+\frac{\partial}{\partial t}\frac{\partial\Phi_r'}{\partial r}=0 \tag{12}$$

For the inner tube

$$\Phi_r=\int_r^b\frac{2I_x}{x}\,dx+2I\log\frac{a'}{b}+\int_{a'}^{b'}\frac{2(I+I_x')}{x}\,dx \tag{13}$$

where

$$I_x=\int_a^x 2\pi i_r r dr \text{ and } I_x'=\int_{a'}^x 2\pi i_r' r dr$$

For $r>b'$, $\Phi_r=0$. Differentiating eq 13 with respect to r

$$\frac{\partial\Phi_r}{\partial r}=-\frac{2I_r}{r}=-\frac{2}{r}\int_a^r 2\pi i_r r dr \tag{14}$$

Similarly for the outer tube,

$$\Phi_r'=\int_r^{b'}\frac{2(I+I_x')}{x}\,dx \tag{15}$$

and

$$\frac{\partial\Phi_r'}{\partial r}=-\frac{2(I+I_x')}{r}=-\frac{2}{r}\left[I+\int_{a'}^r 2\pi i_r' r dr\right]=+\frac{2}{r}\int_r^{b'}2\pi i_r' r dr \tag{16}$$

since $I=-\int_{a'}^{b'}2\pi i_r' r dr$

Inserting eq 14 in eq 11 and eq 16 in eq 12,

$$r\frac{\partial i_r}{\partial r}=\frac{4\pi}{\rho}\frac{\partial}{\partial t}\int_a^r i_r r dr \tag{17}$$

$$r\frac{\partial i_r'}{\partial r}=-\frac{4\pi}{\rho'}\frac{\partial}{\partial t}\int_r^{b'} i_r' r dr \tag{18}$$

Differentiating again with respect to r

$$r\frac{\partial^2 i_r}{\partial r^2}+\frac{\partial i_r}{\partial r}-\frac{4\pi}{\rho}r\frac{\partial i_r}{\partial t}=0 \tag{19}$$

$$r\frac{\partial^2 i_r'}{\partial r^2}+\frac{\partial i_r'}{\partial r}-\frac{4\pi}{\rho'}r\frac{\partial i_r'}{\partial t}=0 \tag{20}$$

If $i_r=I_0\epsilon^{j\omega t}$

$$\frac{\partial}{\partial t}i_r=+j\omega i_r$$

and eq 19 and 20 become

$$\frac{\partial^2 i_r}{\partial r^2}+\frac{1}{r}\frac{\partial i_r}{\partial r}+K^2 i_r=0 \tag{21}$$

$$\frac{\partial^2 i_r'}{\partial r^2}+\frac{1}{r}\frac{\partial i_r'}{\partial r}+K'^2 i_r'=0 \tag{22}$$

where $K^2=-j\omega\frac{4\pi}{\rho}$ and $K'^2=-j\omega\frac{4\pi}{\rho'}$, the solution of eq 21 is

$$i_r=Z_0(Kr)=C_1J_0(Kr)+C_2N_0(Kr) \tag{23}$$

where J_0 and N_0 are Bessel's functions of order 0 and of the first and second kind. C_1 and C_2 are constants of integration. Similarly the solution to eq 22 is

$$i_r'=Z_0'(K'r)=C_1'J_0(K'r)+C_2'N_0'(K'r) \tag{24}$$

The total current is

$$I=2\pi\int_a^b i_r r dr=2\pi\int_a^b rZ_0(Kr)dr \tag{25}$$

and from the general relation

$$\int xZ_0(\alpha x)dx=\frac{1}{\alpha}xZ_1(\alpha x) \tag{26}$$

it follows that

$$I=\frac{2\pi}{K}[bZ_1(Kb)-aZ_1(Ka)] \tag{27}$$

Similarly

$$I'=\frac{2\pi}{K}[b'Z_1'(K'b')-a'Z_1'(K'a')] \tag{28}$$

Likewise

$$I_x=\frac{2\pi}{K}[xZ_1(Kx)-aZ_1(Ka)] \tag{29}$$

$$I_x'=\frac{2\pi}{K'}\left[xZ_1'(K'x)-a'Z_1'(K'a')\right] \tag{30}$$

To obtain values for the Φ_r's substitute eq 29 and 30 in eq 13 and 15. For the inner tube, after performing the integrations

$$\Phi_r=\frac{4\pi}{K^2}\Big[-Z_0(Kx)\Big]_r^b-\frac{4\pi aZ_1(Ka)}{K}\log\frac{b}{r}+2I\log\frac{b'}{b}+\frac{4\pi}{K'^2}\Big[-Z_0'(K'x)\Big]_{a'}^{b'}-\frac{4\pi a'Z_1'(K'a')}{K'}\log\frac{b'}{a'} \tag{31}$$

For the outer tube

$$\Phi_r'=2I\log\frac{b'}{r}+\frac{4\pi}{K'^2}\Big[-Z_0'(K'x)\Big]_r^{b'}-\frac{4\pi a'Z_1'(K'a')}{K'}\log\frac{b'}{r} \tag{32}$$

The voltage drop in the outer tube is

$$e'=\rho' i_r'+\frac{\partial\Phi_r'}{\partial t}.$$

After substituting and simplifying

$$e'=\rho'\left\{\frac{2j\omega I}{\rho'}\log b'+K'a'Z_1'(K'a')\log b'+Z_0'(K'b')-\log r\left[\frac{2j\omega I}{\rho'}+K'a'Z_1'(K'a')\right]\right\} \tag{33}$$

Since e' is not a function of r, the coefficient of $\log r$ in eq 33 must vanish, this gives

$$Z_1'(K'a')=\frac{K'}{2\pi a'}I \tag{34}$$

This is one relation fixing the coefficients in Z_0'. The other relation is in eq 28. Substituting eq 34 in eq 28 gives

$$Z_1'(K'b')=0. \tag{35}$$

Voltage drop in inner tube is, similarly

$$e=\rho Z_0(Kb)+Ka\rho Z_1(Ka)\log b-Ka\rho Z_1(Ka)\log r+2Ij\omega\log\frac{b'}{b}+\rho'[Z_0'(K'b')-Z_0'(K'a')]+\rho'K'a'Z_1'(K'a')\log\frac{b'}{a'} \tag{36}$$

Coefficient of terms involving r must be zero, therefore

$$Z_1(Ka)=0 \tag{37}$$

Putting eq 37 in eq 27

$$Z_1(Kb)=\frac{KI}{2\pi b} \tag{38}$$

Inserting eq 37 and 34 in eq 36 gives

$$e=\rho Z_0(Kb)-2Ij\omega\log\frac{b}{a'}+\rho'[Z_0'(K'b')-Z_0'(K'a')] \tag{39}$$

The effective four-terminal impedance for a shunt with the potential lead inside the inner tube is

$$z=\frac{e-\frac{\partial}{\partial t}\Phi_a}{I}$$

From eq 31, 34 and 37

$$\frac{\partial \Phi_a}{\partial t}=\rho Z_0(Kb)-\rho Z_0(Ka)+\rho'[Z_0'(K'b')-Z_0'(K'a')]-2j\omega I \log \frac{b}{a'} \tag{40}$$

Subtracting eq 40 from 39

$$e-\frac{\partial}{\partial t}\Phi_a=\rho Z_0(Ka) \quad \text{or} \quad z=\frac{\rho Z_0(Ka)}{I} \tag{41}$$

From eq 24 and 34

$$Z_1'(K'a')=\frac{K'}{2\pi a'}I=C_1'J_1'(K'a')+C_2'N_1'(K'a') \tag{42}$$

From eq 24 and 35

$$Z_1'(K'b')=0=C_1'J_1'(K'b')+C_2'N_1(K'b') \tag{43}$$

From eq 23 and 37

$$Z_1(Ka)=0=C_1J_1(Ka)+C_2N_1(Ka) \tag{44}$$

From eq 23 and 38

$$Z_1(Kb)=\frac{KI}{2\pi b}=C_1J_1(Kb)+C_2N_1(Kb) \tag{45}$$

Solving eq 42, 43, 44, and 45 for the coefficients

$$C_1'=\frac{K'I}{2\pi a'}\frac{N_1(K'b')}{D'}$$

$$C_2'=\frac{K'I}{2\pi a'}\frac{J_1(K'b')}{D'},$$

where $D'=J_1(K'a')N_1(K'b')-J_1(K'b')N_1(K'a')$,

$$C_1=-\frac{KI}{2\pi b}\frac{N_1(Ka)}{D} \tag{46}$$

$$C_2=\frac{KI}{2\pi b}\frac{J_1(Ka)}{D}, \tag{47}$$

where $D=J_1(Ka)N_1(Kb)-J_1(Kb)N_1(ka)$.

From eq 23

$$Z_0(Ka)=C_1J_0(Ka)+C_2N_0(Ka)$$

Using this and putting in values of C_1 and C_2 from eq 46 and 47 eq 41 becomes

$$z=\frac{\rho K}{2\pi b}\left[\frac{N_0(Ka)J_1(Ka)-N_1(Ka)J_0(Ka)}{J_1(Ka)N_1(Kb)-J_1(Kb)N_1(Ka)}\right] \tag{48}$$

Using the general relation

$$N_0(Ka)J_1(Ka)-N_1(Ka)J_0(Ka)=\frac{2}{\pi Ka}$$

eq 48 becomes

$$\therefore z=\frac{\rho}{\pi^2 ab}\frac{1}{J_1(Ka)N_1(Kb)-J_1(Kb)N_1(Ka)} \tag{49}$$

Using the following general relations

$$J_1(Ka)=\sqrt{\frac{2}{\pi Ka}}\left[P_1(Ka)\sin\left(Ka-\frac{\pi}{4}\right)+Q_1(Ka)\cos\left(Ka-\frac{\pi}{4}\right)\right]$$

$$N_1(Kb)=\sqrt{\frac{2}{\pi Kb}}\left[-P_1(Kb)\cos\left(Kb-\frac{\pi}{4}\right)+Q_1(Kb)\sin\left(Kb-\frac{\pi}{4}\right)\right],$$

letting $b-a=d$, and putting in the following approximate values of P_1 and Q_1

$$P_1(Ka)=1+\frac{15}{128K^2a^2}$$

$$Q_1(Ka)=\frac{3}{8Ka}$$

the denominator of eq 49 becomes, for $K^2=-jm^2$

$$D_z=\frac{\sqrt{2ab}(1-j)\pi}{m}\left\{\left[\left(1+j\frac{15}{128m^2a^2}\right)\left(1+j\frac{15}{128m^2b^2}\right)+j\frac{9}{64abm^2}\right]\sin\frac{md}{\sqrt{2}}(1-j)+\right.$$

$$\left.\left[\left(1+j\frac{15}{128m^2a^2}\right)\left(\frac{3+3j}{8mb\sqrt{2}}\right)-\left(1+j\frac{15}{128m^2b^2}\right)\left(\frac{3+3j}{8ma\sqrt{2}}\right)\right]\cos\frac{md}{\sqrt{2}}(1-j)\right\} \tag{50}$$

Most of the terms inside the brackets in eq 50 are negligible if the frequency is much above 60 cycles per second. If $f=1{,}000$ c/s, $\rho\leqq 40{,}000$ (cgs units), $(b\text{-}a)\leqq 0.06$ cm, and $b=a=1$ (approximately), this equation simplifies to

$$D_z=\frac{\sqrt{2ab}(1-j)\pi}{m}\sin\frac{md}{\sqrt{2}}(1-j) \tag{51}$$

Letting $\frac{md}{\sqrt{2}}=\delta$ and putting eq 51 back in eq 49

$$z=\frac{\rho\delta}{2\pi d\sqrt{ab}}\left[\frac{(\sin\delta\cosh\delta+\cos\delta\sinh\delta)+j(\cos\delta\sinh\delta-\sin\delta\cosh\delta)}{(\sin\delta\cosh\delta)^2+(\cos\delta\sinh\delta)^2}\right] \tag{52}$$

where

ρ=resistivity of shunt material in cgs units

a=inner radius of shunt tube in cm

b=outer radius of spread tube in cm

d=thickness of shunt-tube wall in cm

$\omega=2\pi$ times the frequency of the current through the shunt.

z=vector impedance of shunt for values of above quantities used.

The *d-c* resistance of the tube in absohms, for $d<b$ is

$$R_{dc}=\frac{\rho}{2\pi d\sqrt{ab}} \tag{53}$$

and eq 52 becomes

$$z=R_{dc}\delta\left[\frac{(\sin\delta\cosh\delta+\cos\delta\sinh\delta)+j(\cos\delta\sinh\delta-\sin\delta\cosh\delta)}{(\sin\delta\cosh\delta)^2+(\cos\delta\sinh\delta)^2}\right] \tag{54}$$

Equation 54 is very nearly correct for any thin-wall tube when the frequency is above 1,000 cycles per second.

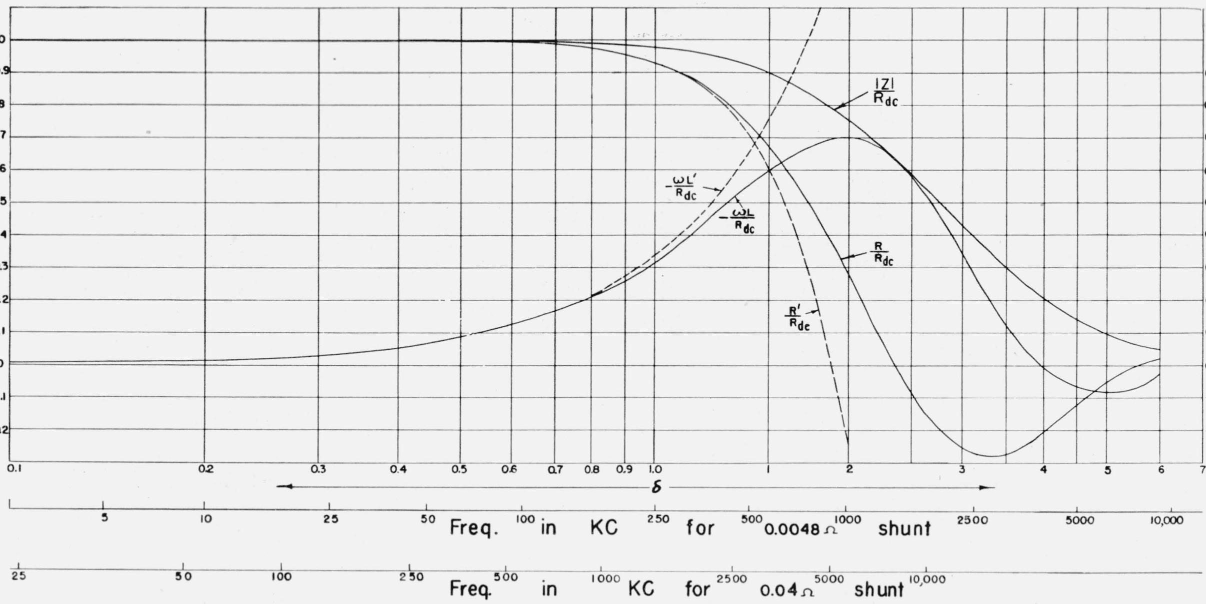

FIGURE 10.—*Curves showing ratios of a-c resistance R, reactance ωL, and impedance Z, to d-c resistance R_{dc}, plotted as ordinates against the parameter, δ, as abscissa.*

Abscissa scales in frequency are also shown for two tubular shunts. The solid-line curves were obtained from the formula derived in appendix 1. The dashed-line curves from formulas known to be applicable only at lower frequencies.

For lower frequencies, the skin effect formula as given on page 91 of Research Paper No. 133 (see reference 5) is

$$R=R_{dc}\left(1-\frac{7m^4d^4}{360}\right)=R_{dc}\left(1-\frac{7}{90}\delta^4\right) \tag{55}$$

The inductance at lower frequencies, where the current is assumed to be uniformly distributed as given on p. 400 of Scientific Paper S281 (see reference 4) is, in abhenries per centimeter,

$$L=-\frac{d}{3a}.$$

For $d<<b$ this gives

$$\frac{\omega L}{R_{dc}}=-\frac{\delta^2}{3} \tag{56}$$

Actual values of R/R_{dc}, $\omega L/R_{dc}$, and $|z|/R_{dc}$ as functions of δ are shown by the curves in figure 10. The solid lines represent values obtained from eq 54 and the broken lines values from eq 55 and 56. For $\delta<1$, the broken and solid curves coincide, but for $\delta>1$ the values obtained from eq 55 and 56 exhibit rapidly increasing errors as would be expected from the assumptions made in the derivation of these equations.

Frequency scales are also given on these curves for the two shunts in use at this laboratory.

2. Magnetic Force Due to Current in a Tube

Referring to figure 9, the magnetic field (H_r) at any point r distance from the axis of the tube, where $a<r>b$, for a total current, I, in abamperes uniformly distributed over the cross section of the tube, is

$$H_r=\frac{r^2-a^2}{b^2-a^2}\,\frac{2I}{r}.$$

The current density inside the metal of the tube is

$$i=\frac{I}{\pi(b^2-a^2)}.$$

The total current in the shell of thickness dr is

$$i_r=i2\pi r dr=\frac{2rI}{b^2-a^2}\,dr.$$

The total radial force (directed inward) on this shell of current, due to the magnetic field H_r is

$$F_r=i_rH_r$$

in dynes per centimeter length of tube. The total force on the entire tube per centimeter of length is

$$F=\int_a^b F_r=\int_a^b \frac{r^2-a^2}{(b^2-a^2)^2}\,4I^2dr$$

Performing the integration

$$F=\frac{4I^2}{(b^2-a^2)^2}\left(\frac{b^3}{3}-a^2b+\frac{2a^3}{3}\right)$$

This force expressed as a pressure per square centimeter is

$$P=\frac{F}{2\pi b}=\frac{2I^2}{\pi b(b^2-a^2)^2}\left(\frac{b^3}{3}-a^2b+\frac{2a^3}{3}\right),$$

which simplifies to

$$P=\frac{2I^2}{3\pi b}\left[\frac{1}{b+a}+\frac{a}{(b+a)^2}\right],$$

which is the pressure in dynes per square centimeter.

The collapsing pressure for thin-wall tubing as obtained from A. E. H. Dove's formula [7] is

$$P_c = \frac{2E}{1-m^2}\left(\frac{t}{D}\right)^3.$$

E is the modulus of elasticity and m is Poisson's ratio for the tube material; t is the wall thickness of the tube and D is its diameter. If E is expressed in dynes per square centimeter, the collapsing pressure P_c will also be in dynes per square centimeter. Equating this to the magnetically induced pressure due to current, I, as obtained above and solving for I, we obtain the current in abamperes at which the tube will collapse

$$I = 1.085\sqrt{\frac{E}{1-m^2}\,\frac{(b-a)^3(b+a)^2}{b^2(b+2a)}}.$$

3. Effective Inductance of a Type I Concentric-Tube Mutual Inductor as a Function of Frequency

In a type I concentric-tube mutual inductor, shown schematically in figure 11, the current, I, whose rate of

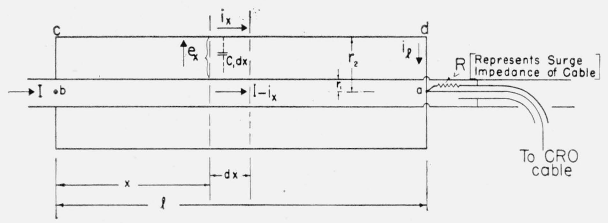

FIGURE 11.—*Schematic drawing of a type I concentric tube mutual inductor.*

change is to be measured, passes through the inner tube and the return circuit for this current is assumed to be far enough away (about 24 in.) so that its effect can be neglected. The secondary circuit of this mutual inductor consists of the length of the inner tube from a to b, the radial ring from b to c, the outer tube from c to d, and the four-wire "spider" from d to a. It is considered to be completed by the resistance, R, which represents the surge impedance of the cable to the CRO. Assuming that (1) all currents flowing in these tubes are uniformly distributed around the central axis, (2) end effects may be neglected, and (3) shunting capacitance from the outer tube to outside conductors may be neglected, differential equations can be written giving the relations of the currents in the tubes to the voltage difference between the tubes at any longitudinal distance, x, from the end of the outer tube. Using symbols defined as follows:

M_1 = mutual inductance per centimeter length of the inner tube, between it and the secondary circuit. Its value is very nearly the same as the self-inductance of the secondary circuit if the wall thickness of each tube is small.

C_1 = capacitance per centimeter length between the inner and outer tubes,

e_x = the potential difference between the inner and outer tubes at the distance, x, from the end of the outer tube,

i_x = the current in the outer tube at the distance x from the end of the outer tube.

the differential equations are

$$di_x = j\omega C_1 e_x dx \tag{57}$$

and

$$de_x = j\omega M_1(I-i_x)dx. \tag{58}$$

The solution of these differential equations gives equations for i_x and e_x containing two arbitrary constants:

$$e_x = K_1 \sinh\left[\omega x\sqrt{C_1M_1} + K_2\right] \tag{59}$$

$$i_x = I + jK_1\sqrt{\frac{C_1}{M_1}}\cosh\left[\omega x\sqrt{C_1M_1} + K_2\right] \tag{60}$$

To obtain values for the arbitrary constants K_1 and K_2, use relations at $x=0$ and $x=l$. At $x=0$, $e_x=0$ and from eq 59

$$0 = K_1 \sinh\left[0 + K_2\right].$$

As K_1 cannot be zero, $K_2=0$.
At $x=l$, $e_x = i_lR$, and from eq 59

$$K_1 = \frac{i_lR}{\sinh \omega l\sqrt{C_1M_1}}.$$

Putting values of K_1 and K_2 in eq 60

$$i_x = I + j\frac{i_lR}{\sinh \omega l\sqrt{C_1M_1}}\sqrt{\frac{C_1}{M_1}}\cosh \omega x\sqrt{C_1M_1}$$

at $x=l$

$$i_l\left[1 - jR\sqrt{\frac{C_1}{M_1}}\,\frac{1}{\tanh \omega l\sqrt{C_1M_1}}\right] = I \tag{61}$$

To get a relation between the voltage impressed on the CRO cable (i_lR) and the rate of change of the current being measured (dI/dt), multiply eq 61 by $j\omega M_1 l$ and take R out of the brackets

$$i_lR\left[\frac{j\omega M_1 l}{R} + \omega M_1 l\sqrt{\frac{C_1}{M_1}}\,\frac{1}{\tanh \omega l\sqrt{C_1M_1}}\right] = j\omega M_1 lI.$$

As $M_1l = M$, the total mutual inductance, the above equation becomes

$$\frac{i_lR}{M}\left[\frac{\omega l\sqrt{M_1C_1}}{\tanh \omega l\sqrt{M_1C_1}} + j\frac{\omega M}{R}\right] = j\omega I. \tag{62}$$

In this equation i_lR is the voltage impressed on the cable going to the CRO and thus is equal to the voltage recorded by the CRO. The value of M is constant and may be computed from the dimensions of the mutual inductor. The right-hand side of this equation is the rate of change of the current, I, being measured. The quantity in the brackets is unity for all but the higher frequencies. Thus, for most surge work the rate of change of the current being measured is obtained by dividing the voltage recorded at the CRO by the constant M. In order to determine the upper limit of frequency for which this relation holds, the magnitude of the vector quantity in the bracket must be

[7] Taken from Marks' Handbook for Mechanical Engineers, Fourth Edition, p. 450.

evaluated as a function of frequency. When the hyperbolic tangent is replaced by the first two terms in its series expansion the magnitude of this quantity becomes:

$$1+\omega^2\left(\frac{M_1C_1l^2}{3}+\frac{M^2}{2R^2}\right).$$

As shown by eq 5 and 6 in the main part of this paper, the product $M_1C_1=1.11\times10^{-21}$ and is the same for any pair of coaxial tubes provided they have thin walls. l is the length of the secondary circuit tube in centimeters. M is the total mutual inductance of the inductor in henries and can be computed from its dimensions as already shown in the main part of this paper. R is the surge impedance in ohms of the cable connected to the potential terminals of the inductor and going to the CRO where it is terminated by a resistance equal to R.

For the type I concentric-tube mutual inductor constructed and used at this laboratory $l=17.8$ cm and $M=0.05\mu$h. The surge impedance of the CRO cable, R, is 50 ohms. For these particular values, the magnitude of the quantity in the brackets of eq 62 varies with frequency as follows:

Frequency	
c/sec.	
30×10^6	1.02
40	1.03_8
50	1.06
60	1.08_6
70	1.11_7
80	1.15_0

For this example of a type I concentric-tube mutual inductor, the rate of change of current as measured at the CRO will be correct to within 10 percent for all frequencies up to about 65 megacycles.

4. Effective Inductance of a Type II Concentric-Tube Mutual Inductor as a Function of Frequency

In a type II concentric-tube mutual inductor as shown schematically in figure 12 the current, I, whose rate of change is to be measured passes through the inner tube (radius r_1) and returns through the outer tube (radius r_3). With this arrangement the current terminals are close together and the self-inductance of the primary current circuit is fixed and quite small. The secondary circuit of this mutual inductor is the same as that of the type I inductor. Making the same assumptions as stated in appendix 3, differential equations can be written giving the relations between currents in the three tubes and voltage differences between the tubes at any longitudinal distance, x, from the end of the middle tube (radius r_2). Using symbols defined as follows:

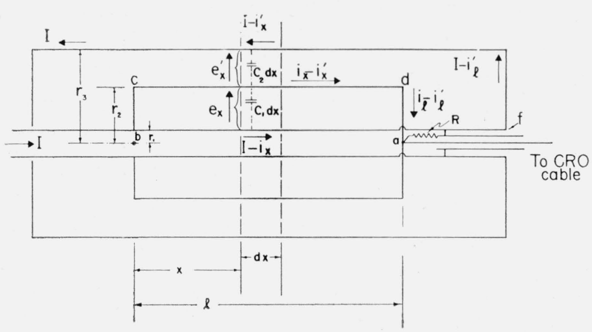

FIGURE 12.—*Schematic drawing of a type* II *concentric tube mutual inductor*

M_1=mutual inductance per centimeter length of the inner tube, between it and the secondary circuit. This is the same as the self-inductance of the secondary circuit if the wall thickness of each tube is small,

L_2=self-inductance per cm of the circuit formed by the middle and outer tubes,

C_1=capacitance per cm between the inner and middle tubes,

C_2=capacitance per cm between the middle and outer tubes,

e_x=the potential difference between the inner and middle tubes at distance, x, from the end of the middle tube,

e'_x=the potential difference between the middle and outer tubes at distance, x, from the end of the middle tube,

i_x=that part of the current flowing at x in the middle tube whose return path is in the inner tube,

i'_x=that part of the current flowing at x in the middle tube whose return path is in the outer tube,

L_0=self-inductance of the circuit formed by the inner and outer tubes from a to f. The differential equations are

$$di_x=j\omega C_1e_xdx \tag{63}$$

$$di'_x=j\omega C_2e'_xdx \tag{64}$$

$$de_x=j\omega M_1(I-i_x)dx \tag{65}$$

$$de'_x=-j\omega L_2(I-i'_x)dx. \tag{66}$$

The solutions of eq 63 and 65 are

$$e_x=K_1\sinh\,[\omega x\sqrt{C_1M_1}+K_2] \tag{67}$$

and

$$i_x=I+jK_1\sqrt{\frac{C_1}{M_1}}\cosh\,[\omega x\sqrt{C_1M_1}+K_2] \tag{68}$$

The solutions of eq 64 and 66 are

$$e'_x=K_3\sin\,[\omega x\sqrt{L_2C_2}+K_4] \tag{69}$$

$$i'_x=I-jK_3\sqrt{\frac{C_2}{L_2}}\cos\,[\omega x\sqrt{L_2C_2}+K_4]. \tag{70}$$

The arbitrary constants K_1, K_2, K_3, and K_4 in the above equations can be determined by using the terminal conditions at $x=0$ and $x=l$.

At $x=0$, $e_x=0$, and $i_x'=0$. So from eq 67

$$0=K_1\sinh\,[0+K_2],$$

but K_1 cannot be zero, therefore $K_2=0$. Also, from eq 70

$$0=I-jK_3\sqrt{\frac{C_2}{L_2}}\cos K_4$$

giving

$$K_3=-j\sqrt{\frac{L_2}{C_2}}\frac{I}{\cos K_4}$$

At $x=l: e_x=R(i_l-i_l')$ and $e_x'=R(i_l-i_l')+j\omega L_0(I-i_l')$.

So from eq 67, after putting in value of K_2,

$$K_1=\frac{R(i_l-i_l')}{\sinh \omega l\sqrt{C_1M_1}}$$

Also, from eq 69, after putting in value of K_3

$$\tan K_4=-\tan \omega l\sqrt{L_2C_2}+\frac{j\sqrt{\frac{C_2}{L_2}}}{I\cos \omega l\sqrt{C_2L_2}}[R(i_l-i_l')+j\omega L_0(I-i_l')].$$

Using above values of K_1 and K_2 eq 68 at $x=l$ gives

$$i_l=I+jR(i_l-i_l')\sqrt{\frac{C_1}{M_1}}\frac{1}{\tanh \omega l\sqrt{M_1C_1}} \tag{71}$$

Using above values of K_3 and K_4 eq 70 at $x=l$ gives

$$i_l'=I-\frac{I}{\cos \omega l\sqrt{C_2L_2}}+j\sqrt{\frac{C_2}{L_2}}\tan \omega l\sqrt{L_2C_2}\,[R(i_l-i_l')+j\omega L_0(I-i_l')] \tag{72}$$

Subtracting eq 72 from eq 71 and assuming i_l' to be very small compared to I in the $j\omega L_0$ term, a value for R $(i-i')$, the voltage across the CRO cable, is obtained

$$(i_l-i_l')R\left[\frac{\frac{\omega l\sqrt{M_1C_1}\cos \omega l\sqrt{L_2C_2}}{\tanh \omega l\sqrt{M_1C_1}}-\omega M_1 l\sqrt{\frac{C_2}{L_2}}\sin \omega l\sqrt{L_2C_2}+j\frac{\omega M_1 l}{R}\cos \omega l\sqrt{L_2C_2}}{1+\omega L_0\sqrt{\frac{C_2}{L_2}}\sin \omega l\sqrt{L_2C_2}}\right]=j\omega M_1 lI$$

For concentric-tubular construction, if the wall thickness of the tubes is neglected the product of capacitance and inductance per cm is a constant for any two tubes. So let $\sqrt{M_1C_1}=\sqrt{L_2C_2}=a=3.33\times10^{-11}$. Also let $M_1l=M$, the total mutual inductance, then the above equation becomes

$$(i_l-i_l')R\left[\frac{\frac{\omega al\cos \omega al}{\tanh \omega al}-\omega M\sqrt{\frac{C_2}{L_2}}\sin \omega al+j\frac{\omega M}{R}\cos \omega al}{1+\omega L_0\sqrt{\frac{C_2}{L_2}}\sin \omega al}\right]=j\omega MI$$

By expanding the first term in the numerator of the quantity in the brackets in series form and neglecting higher order terms, the equation becomes

$$\frac{(i_l-i_l')R}{M}\left[\frac{1-\frac{(\omega al)^2}{6}-\omega M\sqrt{\frac{C_2}{L_2}}\sin \omega al+j\frac{\omega M}{R}\cos \omega al}{1+\omega L_0\sqrt{\frac{C_2}{L_2}}\sin \omega al}\right]=j\omega I \tag{73}$$

This equation is similar to eq 62 of appendix 3 for a type I mutual inductor. Thus, to determine the upper limit of frequency for which a type II inductor can be used, the magnitude of the vector quantity in the brackets of eq 73 must be evaluated as a function of frequency.

A type II mutual inductor having the following dimensions (see fig. 12):

$r_1=0.5$ in.
$r_2=1.0$ in.
$r_3=2$ in.
$l=7$ in.
distance from a to $f=2.5$ in.

is used as an example. By use of eq 5 and 6 in the main part of this paper values for M_1 L_2, C_2, and L_0 may be computed from these dimensions. Then, assuming the CRO cable surge impedance, R, to be 50 ohms, the magnitude of the quantity in the bracket of eq 73 varies with frequency as follows:

Frequency	
c/sec	
10×10^6	0.998
30	.982
50	.952
60	.932
70	.908
80	.885
90	.861
100	.835

For this example of a type II concentric-tube mutual inductor the rate of change of current as measured at the CRO will be correct to within 10 percent for all frequencies up to 70 megacycles.

WASHINGTON, March 28, 1947.